

2011

Electron and Hydride Addition to Gold (I) Thiolate Oligomers: Implications for Gold–Thiolate Nanoparticle Growth Mechanisms

Brian M. Barngrover

Stephen F Austin State University, barngrovbm@sfasu.edu

Christine M. Aikens

Follow this and additional works at: http://scholarworks.sfasu.edu/chemistry_facultypubs

 Part of the [Chemistry Commons](#)

Tell us how this article helped you.

Recommended Citation

Barngrover, Brian M. and Aikens, Christine M., "Electron and Hydride Addition to Gold (I) Thiolate Oligomers: Implications for Gold–Thiolate Nanoparticle Growth Mechanisms" (2011). *Faculty Publications*. Paper 54.

http://scholarworks.sfasu.edu/chemistry_facultypubs/54

This Article is brought to you for free and open access by the Chemistry and Biochemistry at SFA ScholarWorks. It has been accepted for inclusion in Faculty Publications by an authorized administrator of SFA ScholarWorks. For more information, please contact cdsscholarworks@sfasu.edu.

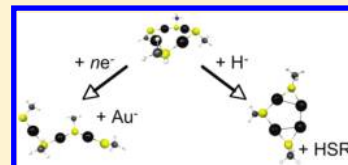
Electron and Hydride Addition to Gold(I) Thiolate Oligomers: Implications for Gold–Thiolate Nanoparticle Growth Mechanisms

Brian M. Barngrover and Christine M. Aikens*

Department of Chemistry, Kansas State University, 213 CBC Building, Manhattan, Kansas 66506, United States

S Supporting Information

ABSTRACT: Electron and hydride addition to Au(I):SR oligomers is investigated using density functional theory. Cyclic and chain-like clusters are examined in this work. Dissociation to Au[−] ions and Au_n(SR)_{n+1}[−] chains is observed after 2–4 electrons are added to these systems. The free thiolate (SR[−]) is rarely produced in this work; dissociation of Au[−] is preferred over dissociation of SR[−]. Electron affinities calculated in gas phase, toluene, and water suggest that the electron addition process is unlikely, although it may be possible in polar solvents. In contrast, hydride addition to Au(I):SR oligomers yields free thiols and complexes containing Au–Au bonds, which are plausible intermediates for gold nanoparticle growth. The resulting compounds can react to form larger nanoparticles or undergo further reduction by hydride to yield additional Au–Au bonds.



SECTION: Nanoparticles and Nanostructures

Au(I):SR compounds have been used extensively as antiarthritic and antitumor drugs.¹ They also have a significant impact in nanoscience, since linear –SR–Au–SR– and V-shaped –SR–Au–SR–Au–SR– motifs are present on the surfaces of gold nanoparticles including Au₂₅(SR)₁₈^{0,−1}, Au₃₈(SR)₂₄, and Au₁₀₂(SR)₄₄ (refs 2–8) as well as self-assembled monolayers (SAMs) (refs 9–11). Longer chain-like oligomers such as Au₃(SR)₄[−] have been proposed to passivate smaller nanoclusters.^{12,13} 1:1 (AuSR)_n systems have also been observed experimentally, and the structures of these systems are often cyclic or helical.^{14–17}

Gold(I) thiolate oligomers can be generated under gold nanoparticle growth conditions and have been suggested to play an important role in the growth mechanism,^{18–21} although recent mechanistic investigations draw this into question.²² Since the initial two-phase synthesis of thiol(ate)-stabilized gold nanoparticles by Brust et al.,²³ many researchers have examined the role of a variety of variables on growth (see ref 24 and references therein). Solvents such as toluene, methanol, and tetrahydrofuran (THF) are commonly used.^{19,21,23,24} Schaaff et al. found that a 3:1 ratio of thiol to gold salt as well as a great molar excess of the reducing agent NaBH₄ are required to obtain smaller nanocrystals.¹⁹ Of note, Murray and co-workers utilize a “modified Brust” synthesis in which a 10× molar excess of NaBH₄ is used to reduce the gold salt.²⁵ Other reducing agents such as 9-BBN can also be employed.²⁶ However, not all syntheses require a reducing agent; an electrochemical procedure has also been reported.²⁷

Previous work in our group on the mechanisms of gold-phosphine cluster growth from AuPR₃Cl precursors has shown that the gain of one electron is required to initiate Au–Au bond formation, while additional electrons lead to spontaneous Cl[−] dissociation.²⁸ If a similar mechanism is involved in gold–thiolate growth, SR[−] dissociation upon addition of multiple electrons would be expected.

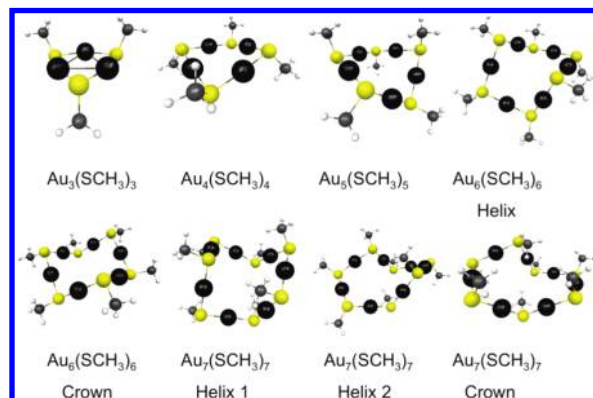


Figure 1. Cyclic Au_n(SCH₃)_n (*n* = 3–7) clusters. Gold: black; sulfur: yellow; carbon: gray; hydrogen: white.

In order to examine the growth mechanisms of gold–thiolate nanoparticles, cyclic gold methylthiolate structures with stoichiometries ranging from Au₃(SCH₃)₃ to Au₇(SCH₃)₇ have been optimized at the BP86/TZP level of theory in the gas phase (Figure 1). These structures are comparable to those previously reported with other levels of theory.^{29–32}

In order to examine the possibility of electron-driven Au–Au bond formation and spontaneous SCH₃[−] dissociation, one to four electrons are added to each cluster and the system is allowed to relax. For Au₃(SCH₃)₃ through Au₇(SCH₃)₇, the addition of a single electron leads to a slight flattening of the structure, but no

Received: March 7, 2011

Accepted: April 7, 2011

Published: April 11, 2011

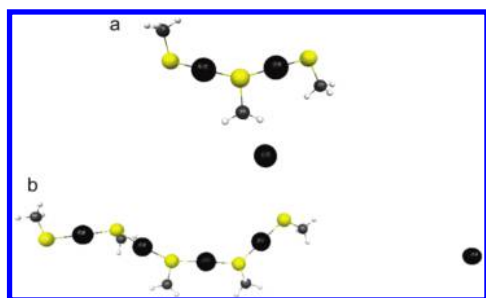


Figure 2. (a) Dissociation of Au^- from $\text{Au}_3(\text{SCH}_3)_3$ after addition of two electrons. (b) Dissociation of Au^- from $\text{Au}_5(\text{SCH}_3)_5$ after addition of three electrons.

Table 1. Vertical EAs in eV for Gold-Thiolate Oligomers in the Gas Phase

	first EA	second EA	third EA
<i>cyclic</i>			
$\text{Au}_3(\text{SCH}_3)_3$	-0.30	1.49	^a
$\text{Au}_4(\text{SCH}_3)_4$	-0.20	2.39	5.59
$\text{Au}_5(\text{SCH}_3)_5$	-0.31	1.93	4.89
$\text{Au}_6(\text{SCH}_3)_6$ crown	-0.78	1.55	4.30
$\text{Au}_6(\text{SCH}_3)_6$ helix	-0.53	1.55	4.24
$\text{Au}_7(\text{SCH}_3)_7$ crown	-0.69	1.68	^a
$\text{Au}_7(\text{SCH}_3)_7$ helix 1	-0.56	1.65	3.62
$\text{Au}_7(\text{SCH}_3)_7$ helix 2	-0.56	1.54	3.71
<i>chain-like</i>			
$\text{Au}_3(\text{SCH}_3)_3$ gold-capped	-2.63	2.06	^a
$\text{Au}_2(\text{SCH}_3)_3^-$	3.51	5.81	^a
$\text{Au}_3(\text{SCH}_3)_4^-$	2.90	4.68	^a

^a Gold dissociated after second electron addition.

dissociation occurs. For the highly strained $\text{Au}_3(\text{SCH}_3)_3$ system, addition of two electrons leads to dissociation of a Au^- ion and formation of a $\text{Au}_2(\text{SCH}_3)_3^-$ anionic chain structure (Figure 2a). However, $\text{Au}_n(\text{SCH}_3)_n$ systems with $n > 3$ generally do not dissociate when two electrons are added to the neutral cyclic cluster. Most systems require the addition of three electrons before dissociation to m ($m = 1-2$) Au^- ions and a chain-like $\text{Au}_m(\text{SCH}_3)_m^-$ species occurs. As an example, the dissociation products for the $\text{Au}_5(\text{SCH}_3)_5$ cluster with three electrons are shown in Figure 2b. A subset of systems has also been studied with the addition of four electrons; in these cases the dissociation products are two anionic chains and 2 Au^- ions. In the systems examined here, gold is released as Au^- rather than $\text{Au}(0)$, and the gold ions are unlikely to form nanoparticles due to Coulomb repulsion.

Vertical electron affinities (EAs) are calculated for optimized structures that have accepted 0–3 additional electrons. As shown in Table 1, the first EA is calculated to be -0.20 to -0.78 eV and the EAs generally increase with the size of the cluster although this trend is not monotonic. In consequence, it is favorable for the system to gain one electron. However, the EAs for clusters that have already accepted one electron lie in the range of +1.49–2.39 eV. EAs for a third electron are even less favorable at +3.62–5.60 eV. Due to self-interaction error in density functional theory, EAs are normally predicted to be less positive/more negative than the true values; for our systems, this

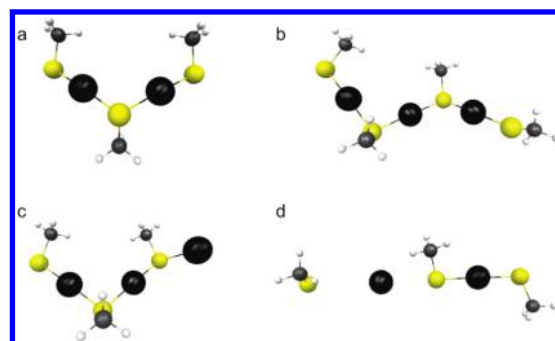


Figure 3. (a) $\text{Au}_2(\text{SCH}_3)_3^-$. (b) $\text{Au}_3(\text{SCH}_3)_4^-$. (c) Gold-capped $\text{Au}_3(\text{SCH}_3)_3$. (d) $\text{Au}_2(\text{SCH}_3)_3^-$ dissociation into a Au^- ion, a SCH_3^- ligand, and a $\text{Au}(\text{SCH}_3)_2^-$ complex.

Table 2. Vertical EAs in eV of Cyclic $\text{Au}_n(\text{SCH}_3)_n$ in Water and Toluene

	water			toluene		
	first EA	second EA	third EA	first EA	second EA	third EA
$\text{Au}_3(\text{SCH}_3)_3$	-2.19	-3.87	^a	-1.35	-1.53	^a
$\text{Au}_4(\text{SCH}_3)_4$	-1.92	-2.36	^a	-1.16	-0.28	0.95
$\text{Au}_5(\text{SCH}_3)_5$	-1.97	-2.45	^a	-1.17	-0.51	1.08
$\text{Au}_6(\text{SCH}_3)_6$ crown	-2.01	-2.48	^a	-1.40	-0.71	0.72
$\text{Au}_6(\text{SCH}_3)_6$ helix	-1.98	-2.49	^a	-1.33	-0.69	0.68
$\text{Au}_7(\text{SCH}_3)_7$ crown	-1.93	-2.32	-1.62	-1.39	-0.49	0.51
$\text{Au}_7(\text{SCH}_3)_7$ helix 1	-1.85	-2.44	-2.20	-1.25	-0.52	0.33
$\text{Au}_7(\text{SCH}_3)_7$ helix 2	-1.92	-2.50	^a	-1.33	-0.63	0.37

^a Gold dissociated after second electron addition.

would further decrease the likelihood that a cluster will gain additional electrons. MP2 calculations have been performed on a subset of the systems, and the EAs are shown to be more positive with this level of theory (see Table S1 in the Supporting Information). Overall, it does not seem likely that these $\text{Au}(\text{I})$:SR cyclic clusters can acquire enough charge to lead to dissociation, although it should be noted that a significant excess of reducing agent is present under experimental growth conditions.

Because the $\text{Au}(\text{I})$:SR oligomers created during the growth process may not be cyclic, $\text{Au}(\text{I})$:SR chains have also been examined in this work. The $\text{Au}_2(\text{SCH}_3)_3^-$ anionic chain structure and related $\text{Au}_3(\text{SCH}_3)_4^-$ chain are examined in addition to a chain-like $\text{Au}_3(\text{SCH}_3)_3$ system (Figure 3). The EAs for the anionic chain clusters are highly positive (2.90–3.51 eV for the first electron; 4.68–5.81 for the second). Upon the addition of two electrons, the $\text{Au}_2(\text{SCH}_3)_3^-$ cluster dissociates into a Au^- ion, SCH_3^- ligand, and $\text{Au}(\text{SCH}_3)_2^-$ complex (Figure 3d). The first EA for the neutral chain-like $\text{Au}_3(\text{SCH}_3)_3$ system is strongly negative at -2.63 eV. However, the second EA lies at 2.06 eV, which is in the range of second EAs for other neutral clusters. Upon relaxation of the structure with two additional electrons, the terminal gold atom dissociates as Au^- , while the remaining cluster is the commonly observed $\text{Au}_2(\text{SCH}_3)_3^-$ chain. It should be noted that no individual thiolates dissociate in this process, so dissociation of Au^- is preferred over dissociation of SCH_3^- .

Because EAs are affected by solvation, the electron addition process is also examined in toluene and in water. EAs calculated in these solvents are shown in Table 2. As a highly polar solvent, water is expected to stabilize complexes with a greater additional charge. In both solvents, addition of the first electron is highly

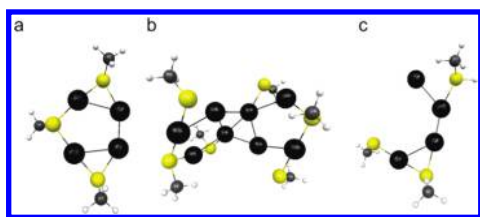


Figure 4. (a) $\text{Au}_4(\text{SCH}_3)_3^-$ product from hydride addition to $\text{Au}_4(\text{SCH}_3)_4$. (b) $\text{Au}_8(\text{SCH}_3)_6^{2-}$ formed from two $\text{Au}_4(\text{SCH}_3)_3^-$ complexes. (c) Second hydride addition to $n = 4$ product.

avored by all clusters. The EAs range from -1.16 to -1.39 eV for toluene and from -1.85 to -2.18 eV for water. The addition of a second electron in toluene is less favored than the addition of the first electron; however, in water the second addition is more favored than the first addition. These EAs range from -0.28 to -0.71 eV for toluene and from -2.32 to -2.49 eV for water, with the exception of $\text{Au}_3(\text{SCH}_3)_3$ for which the first and second EAs are more negative. Addition of the second electron is favorable in both solvents for all systems examined here.

As in the gas phase, addition of two electrons to $\text{Au}_3(\text{SCH}_3)_3$ in both toluene and water leads to the loss of Au^- . However, in contrast to the gas phase, in water only two electrons are required to lead to dissociation of all $\text{Au}_n(\text{SCH}_3)_n$ species except the crown and helix 1 isomers of $\text{Au}_7(\text{SCH}_3)_7$. The larger species may be better able to stabilize additional charge. Three electrons are still required for dissociation of $\text{Au}_n(\text{SCH}_3)_n$ ($n = 4-7$) in toluene; however, the third EA of these systems is positive, suggesting that the addition of this electron is unfavorable. Just as before, the species generated by dissociation are gold ions and anionic chain complexes. A nanoparticle growth mechanism involving these species would be quite involved, since the gold would need to be oxidized before larger nanoparticles could be formed due to Coulombic repulsion between Au^- ions.

Because straightforward addition of electrons does not lead to a plausible mechanism for growth and since the NaBH_4 reducing agent can act as a hydride donor, we have also examined hydride addition to the cyclic $\text{Au}_n(\text{SCH}_3)_n$ species. Depending on the angle of the incoming hydride, different products can be formed. For H-S-C angles of approximately 180° , a ligand exchange occurs in which CH_3^- is released to leave a cyclic $\text{Au}_n(\text{SH})(\text{SCH}_3)_{n-1}$ species. When the hydride reacts at an angle closer to 120° , HSCH_3 dissociates from the cluster, and the two gold atoms originally bound to the sulfur of the leaving thiol form a Au-Au bond. To illustrate this bond formation, the $n = 4$ product is shown in Figure 4a. This system has a -1 charge overall. Since the V-shaped $-\text{SR-Au-SR-Au-SR-}$ motif typically has a -1 charge, the two Au atoms involved in the bond are formally $\text{Au}(0)$. The highest occupied molecular orbital (HOMO) of this system is a σ orbital. Similar products are observed for all reactants with $n = 3-7$. Once Au-Au bonds have formed, two units such as $\text{Au}_4(\text{SCH}_3)_3^-$ will bind to form a stable $\text{Au}_8(\text{SCH}_3)_6^{2-}$ species, even though this leads to a higher overall charge (Figure 4b). This cluster contains 4 $\text{Au}(0)$ atoms in the center surrounded by two $\text{Au}_2(\text{SCH}_3)_3^-$ units, which suggests that nanoparticle growth could proceed in this manner. A similar neutral $\text{Au}_8(\text{SCH}_3)_6$ cluster was optimized previously using density functional theory, and the authors suggested that this cluster may be subject to further reactions since the core is quite open.³³ Since further addition of $\text{Au}_4(\text{SCH}_3)_3^-$ units to $\text{Au}_8(\text{SCH}_3)_6^{2-}$ would lead to charge build-up, mechanisms for

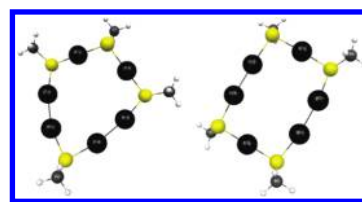


Figure 5. Two products formed after the addition of two hydrides to $\text{Au}_6(\text{SCH}_3)_6$.

charge removal (such as anionic ligand dissociation or electron transfer) will need to be considered in the future.

Addition of a hydride effectively adds two electrons to the gold-thiolate cluster. Thus, after the first hydride reaction, two electrons are available for gold-gold bonding. (It should be noted that, although hydride is a two-electron donor, the dissociation products obtained are very different compared to those from the two-electron addition process.) After a second hydride addition, four electrons would be available for bonding (assuming a free thiol is released as before). For the smallest systems examined here, this is greater than the number of Au atoms that can form Au-Au bonds, since some gold atoms remain between two thiolates. As a consequence, addition of a second hydride to $\text{Au}_4(\text{SCH}_3)_3^-$ results in no reaction if the hydride is added to the thiolate at the apex of the V, or opens the cluster as shown in Figure 4c if added at the corners. However, for larger systems such as $n = 6$, new Au-Au bonds are formed during the second hydride reaction. Different structures are formed depending on hydride addition location as illustrated in Figure 5. Alternatively, hydride addition to gold is possible. In this case, no additional Au-Au bonds are formed.

In summary, addition of a hydride ion to gold-thiolate oligomers leads to products including free thiols and compounds that contain both $\text{Au}(0)$ and chain-like oligomers $\text{Au}_n(\text{SR})_{n+1}^-$ ($n = 1-6$), which are plausible intermediates for gold nanoparticle growth. In contrast, addition of electrons leads to the formation of isolated Au^- ions and $\text{Au}_n(\text{SR})_{n+1}^-$ chains, whereas formation of the free thiolate SR^- is almost never observed in this work. Although electron addition to yield anionic species may be possible in water, it is not favorable in the gas phase or in common organic solvents such as toluene. In addition, a nanoparticle growth mechanism involving these species would be quite involved, as the gold atoms would subsequently need to be oxidized before larger gold nanoparticles could be formed. Overall, assuming that nanoparticle growth proceeds via reduction of $\text{Au}_n(\text{SR})_n$ oligomers, it is likely to be initiated by hydride addition to an SR group leading to Au-Au bond formation and HSR dissociation.

COMPUTATIONAL DETAILS

The Amsterdam density functional program (ADF)³⁴ was employed for all calculations in this work. A polarized triple- ζ (TZP) basis set is used with a $[1s^2-4f^{14}]$ frozen core for gold, a $[1s^2-2p^6]$ frozen core for sulfur, and a $[1s^2]$ frozen core for carbon. The generalized gradient approximation (GGA) Becke-Perdew (BP86)^{35,36} exchange-correlation functional is used in structure relaxations. Scalar relativistic effects are incorporated by adopting the zero-order regular approximation (ZORA).³⁷ The conductor-like screening model (COSMO)³⁸ is employed to include the effects of continuum solvation in the calculations; both toluene and water solvents are considered.

Unrestricted calculations are employed for systems with open-shell electrons. In the electron addition process, both singlet and triplet multiplicities have been considered for initial gas phase calculations. Triplet states were found to be higher energy and were not considered further.

Both Mulliken and Voronoi Deformation Density charges have been examined in order to assign partial charges on dissociating fragments. Au atoms with charges of approximately -1 have been assigned in the main text as Au^- .

Vertical EAs are defined as the energy of reaction for $X + e^- \rightarrow X^-$, where the energy of X^- is calculated at the optimized geometry of X . X^- is fully optimized before the second EA ($X^- + e^- \rightarrow X^{2-}$) is determined. Likewise, X^{2-} is optimized before the third EA is computed.

■ ASSOCIATED CONTENT

S Supporting Information. MP2 and BP86 EA calculations for $\text{Au}_5(\text{SCH}_3)_5$. This material is available free of charge via the Internet <http://pubs.acs.org>.

■ AUTHOR INFORMATION

Corresponding Author

*E-mail: cmaikens@ksu.edu.

■ ACKNOWLEDGMENT

The authors thank the Air Force Office of Scientific Research for funding under Grant FA9550-09-1-0451. C.M.A. is a 2011 Alfred P. Sloan Research Scholar.

■ REFERENCES

- (1) Shaw, C. F., III. Gold-Based Therapeutic Agents. *Chem. Rev.* **1999**, *99*, 2589–2600.
- (2) Jadzinsky, P. D.; Calero, G.; Ackerson, C. J.; Bushnell, D. A.; Kornberg, R. D. Structure of a Thiol Monolayer-Protected Gold Nanoparticle at 1.1 Å Resolution. *Science* **2007**, *318*, 430–433.
- (3) Heaven, M. W.; Dass, A.; White, P. S.; Holt, K. M.; Murray, R. W. Crystal Structure of the Gold Nanoparticle $[\text{N}(\text{C}_8\text{H}_{17})_4][\text{Au}_{25}(\text{SCH}_2\text{CH}_2\text{Ph})_{18}]^-$. *J. Am. Chem. Soc.* **2008**, *130*, 3754–3755.
- (4) Akola, J.; Walter, M.; Whetten, R. L.; Häkkinen, H.; Grönbeck, H. On the Structure of Thiolate-Protected Au_{25} . *J. Am. Chem. Soc.* **2008**, *130*, 3756–3757.
- (5) Zhu, M.; Aikens, C. M.; Hollander, F. J.; Schatz, G. C.; Jin, R. Correlating the Crystal Structure of a Thiol-Protected Au_{25} Cluster and Optical Properties. *J. Am. Chem. Soc.* **2008**, *130*, 5883–5885.
- (6) Zhu, M.; Eckenhoff, W. T.; Pintauer, T.; Jin, R. Conversion of Anionic $[\text{Au}_{25}(\text{SCH}_2\text{CH}_2\text{Ph})_{18}]^-$ Cluster to Charge Neutral Cluster via Air Oxidation. *J. Phys. Chem. C* **2008**, *112*, 14221–14224.
- (7) Lopez-Acevedo, O.; Tsunoyama, H.; Tsukuda, T.; Häkkinen, H.; Aikens, C. M. Chirality and Electronic Structure of the Thiolate-Protected Au_{38} Nanocluster. *J. Am. Chem. Soc.* **2010**, *132*, 8210–8218.
- (8) Qian, H.; Eckenhoff, W. T.; Zhu, Y.; Pintauer, T.; Jin, R. Total Structure Determination of Thiolate-Protected Au_{38} Nanoparticles. *J. Am. Chem. Soc.* **2010**, *132*, 8280–8281.
- (9) Maksymovych, P.; Sorescu, D. C.; Yates, J. T., Jr. Gold-Adatom-Mediated Bonding in Self-Assembled Short-Chain Alkanethiolate Species on the Au(111) Surface. *Phys. Rev. Lett.* **2006**, *97*, 146103.
- (10) Cossaro, A.; Mazzarello, R.; Rousseau, R.; Casalis, L.; Verdini, A.; Kohlmeyer, A.; Floreano, L.; Scandolo, S.; Morgante, A.; Klein, M. L.; X-ray Diffraction and Computation Yield the Structure of Alkanethiols on Gold(111). *Science* **2008**, *321*, 943–946.

- (11) Grönbeck, H.; Häkkinen, H.; Whetten, R. L. Gold–Thiolate Complexes Form a Unique $c(4 \times 2)$ Structure on Au(111). *J. Phys. Chem. C* **2008**, *112*, 15940–15942.

- (12) Jiang, D.-e.; Chen, W.; Whetten, R. L.; Chen, Z. What Protects the Core When the Thiolated Au Cluster is Extremely Small? *J. Phys. Chem. C* **2009**, *113*, 16983–16987.

- (13) Pei, Y.; Gao, Y.; Shao, N.; Zeng, X. C. Thiolate-Protected $\text{Au}_{20}(\text{SR})_{16}$ Cluster: Prolate Au_8 Core with New $[\text{Au}_3(\text{SR})_4]$ Staple Motif. *J. Am. Chem. Soc.* **2009**, *131*, 13619–13621.

- (14) Bau, R. Crystal Structure of the Antiarthritic Drug Gold Thiomalate (Myochrysin): A Double-Helical Geometry in the Solid State. *J. Am. Chem. Soc.* **1998**, *120*, 9380–9381.

- (15) LeBlanc, D. J.; Lock, C. J. L. *cyclo*-Hexakis[(2,4,6-triisopropylthio-phenolato-S:S)gold(I)] Diethyl Ether Solvate. *Acta Cryst. C* **1997**, *53*, 1765–1768.

- (16) Wiseman, M. R.; Marsh, P. A.; Bishop, P. T.; Brisdon, B. J.; Mahon, M. F. Homoleptic Gold Thiolate Catenanes. *J. Am. Chem. Soc.* **2000**, *122*, 12598–12599.

- (17) Simpson, C. A.; Farrow, C. L.; Tian, P.; Billinge, S. J. L.; Huffman, B. J.; Harkness, K. M.; Cliffl, D. E. Tiopronin Gold Nanoparticle Precursor Forms Auophilic Ring Tetramer. *Inorg. Chem.* **2010**, *49*, 10858–10866.

- (18) Alvarez, M. M.; Khoury, J. T.; Schaaff, T. G.; Shafiqullin, M.; Vezmar, I.; Whetten, R. L. Critical Sizes in the Growth of Au Clusters. *Chem. Phys. Lett.* **1997**, *266*, 91–98.

- (19) Schaaff, T. G.; Shafiqullin, M. N.; Khoury, J. T.; Vezmar, I.; Whetten, R. L.; Cullen, W. G.; First, P. N.; Gutiérrez-Wing, C.; Ascensio, J.; Jose-Yacamán, M. J. Isolation of Smaller Nanocrystal Au Molecules: Robust Quantum Effects in Optical Spectra. *J. Phys. Chem. B* **1997**, *101*, 7885–7891.

- (20) Templeton, A. C.; Wuelfing, W. P.; Murray, R. W. Monolayer-Protected Cluster Molecules. *Acc. Chem. Res.* **2000**, *33*, 27–36.

- (21) Negishi, Y.; Nobusada, K.; Tsukuda, T. Glutathione-Protected Gold Clusters Revisited: Bridging the Gap between Gold(I)-Thiolate Complexes and Thiolate-Protected Gold Nanocrystals. *J. Am. Chem. Soc.* **2005**, *127*, 5261–5270.

- (22) Goulet, P. J. G.; Lennox, R. B. New Insights into Brust-Schiffrin Metal Nanoparticle Synthesis. *J. Am. Chem. Soc.* **2010**, *132*, 9582–9584.

- (23) Brust, M.; Walker, M.; Bethell, D.; Schiffrin, D. J.; Whyman, R. Synthesis of Thiol-Derivatized Gold Nanoparticles in a Two-Phase Liquid–Liquid System. *J. Chem. Soc., Chem. Commun.* **1994**, 801.

- (24) Parker, J. F.; Weaver, J. E. F.; McCallum, F.; Fields-Zinna, C. A.; Murray, R. W. Synthesis of Monodisperse $[\text{Oct}_4\text{N}^+][\text{Au}_{25}(\text{SR})_{18}^-]$ Nanoparticles, with Some Mechanistic Observations. *Langmuir* **2010**, *26*, 13650–13654.

- (25) Song, Y.; Harper, A. S.; Murray, R. W. Ligand Heterogeneity on Monolayer-Protected Gold Clusters. *Langmuir* **2005**, *21*, 5492–5500.

- (26) Sardar, R.; Shumaker-Parry, J. S. 9-BBN Induced Synthesis of Nearly Monodisperse ω -Functionalized Alkylthiol Stabilized Gold Nanoparticles. *Chem. Mater.* **2009**, *21*, 1167–1169.

- (27) Nagaraju, D. H.; Lakshminarayanan, V. Electrochemical Synthesis of Thiol-Monolayer-Protected Clusters of Gold. *Langmuir* **2008**, *24*, 13855–13857.

- (28) Guidez, E. B.; Hadley, A.; Aikens, C. M. Initial Growth Mechanisms of Gold-Phosphine Clusters. *J. Phys. Chem. C* **2011**, *115*, 6305–6316.

- (29) Howell, J. A. S. Structure and Bonding in Cyclic Thiolate Complexes of Copper, Silver, and Gold. *Polyhedron* **2006**, *25*, 2993–3005.

- (30) Grönbeck, H.; Walter, M.; Häkkinen, H. Theoretical Characterization of Cyclic Thiolated Gold Clusters. *J. Am. Chem. Soc.* **2006**, *128*, 10268–10275.

- (31) Shao, N.; Pei, Y.; Gao, Y.; Zeng, X. C. Onset of Double Helical Structure in Small-Sized Homoleptic Gold Thiolate Clusters. *J. Phys. Chem. A* **2009**, *113*, 629–632.

- (32) Kacprzak, K. A.; Lopez-Acevedo, O.; Häkkinen, H.; Grönbeck, H. Theoretical Characterization of Cyclic Thiolated Copper, Silver, and Gold Clusters. *J. Phys. Chem. C* **2010**, *114*, 13571–13576.

(33) Jiang, D.-e.; Whetten, R. L.; Luo, W.; Dai, S. The Smallest Thiolated Gold Superatom Complexes. *J. Phys. Chem. C* **2009**, *113*, 17291–17295.

(34) te Velde, G.; Bickelhaupt, F. M.; Baerends, E. J.; Fonseca Guerra, C.; van Gisbergen, S. J. A.; Snijders, J. G.; Ziegler, T. Chemistry with ADF. *J. Comput. Chem.* **2001**, *22*, 931–967.

(35) Becke, A. D. Density-Functional Exchange-Energy Approximation with Correct Asymptotic Behavior. *Phys. Rev. A* **1988**, *38*, 3098.

(36) Perdew, J. P. Density-Functional Approximation for the Correlation Energy of the Inhomogeneous Electron Gas. *Phys. Rev. B* **1986**, *33*, 8822.

(37) van Lenthe, E.; Baerends, E. J.; Snijders, J. G. Relativistic Regular Two-Component Hamiltonians. *J. Chem. Phys.* **1993**, *99*, 4597.

(38) Klamt, A.; Schüürmann, G. COSMO: A New Approach to Dielectric Screening in Solvents with Explicit Expressions for the Screening Energy and Its Gradient. *J. Chem. Soc., Perkin Trans.* **1993**, *2*, 799.